Supporting Information for

Enabling Facile Anionic Kinetics through Cationic Redox Mediator in Li-Rich Layered Cathodes

Ning Li,[1] Jue Wu,[2,3] Sooyeon Hwang,[4] Joseph K. Papp,[5] Wang Hay Kan,[6] Liang Zhang,[2] Chenhui Zhu,[2] Bryan D. McCloskey,[1,5] Wanli Yang,[2*] and Wei Tong[1*]

[1]*Energy Storage and Distributed Resources Division, Lawrence Berkeley National Laboratory Berkeley, CA 94720 USA*

[2]*Advanced Light Source, Lawrence Berkeley National Laboratory Berkeley, CA 94720 USA*

[3]*State Key Laboratory for Physical Chemistry of Solid Surfaces, Department of Chemistry, College of Chemistry and Chemical Engineering, Xiamen University, Fujian 361005 China*

[4] *Center for Functional Nanomaterials, Brookhaven National Laboratory, Upton, NY 11973 USA*

[5] *Department of Chemical and Biomolecular Engineering, University of California, Berkeley, CA 94720 USA*

[6] *Dongguan Neutron Science Center, Dongguan, Guangdong 523803 China*

**Corresponding Author: Wei Tong (weitong@lbl.gov), Wanli Yang (wlyang@lbl.gov)*

Experimental Section

Material Synthesis. Layered Li-rich ruthenium cobalt oxide (LRCO) samples were prepared by mixing the stoichiometric amounts of Li_2CO_3, Co_2O_3, and RuO_2 precursors using a Spex 8000 mill for 3 h, followed by the calcination at 950 or 1000 ºC for designated durations in air.

Physical Characterization. sXRD patterns were taken on beamline 11-BM at Advanced Photon Source at Argonne National Laboratory. The beamline uses a sagittal focused X-ray beam with a high precision diffractometer circle and perfect Si (111) crystal analyzer detection for high sensitivity and resolution. The sXRD data were analyzed by the conventional Rietveld method using the general structure analysis system (GSAS) package with the graphical user interface (EXPGUI).[1] *Ex situ* WAXS patterns were collected on beamline 7.3.3 at a fixed energy of 10,000 eV at Advanced Light Source (ALS). Some powder XRD patterns were collected on a Bruker D2-Phaser with Cu Kα radiation (λ = 1.54178 Å). Hard XAS measurements were performed on beamline 2-2 in a transmission mode using a (220) monochromator at Stanford Synchrotron Radiation Lightsource (SSRL). Higher harmonics in the X-ray beam was reduced by detuning the Si (220) monochromator. Energy calibration was accomplished by using the first inflection points in the spectra of Ni and Ru foil reference. XANES data were analyzed by SIXPACK software with the Photoelectron Energy Origin E_0 determined by the first inflection point of the absorption edge jump. Soft XAS measurements were carried out on beamline endstation 10-1 at SSRL. The Ni L-edge and O K-edge spectra were acquired under ultrahigh vacuum (10-9 Torr) in a single load at room temperature using total electron yield (TEY) via the drain current and fluorescence yield (FY) *via* Silicon Photodiodes. All the cycled electrodes were immediately recovered from the cells at designated cutoff voltages to minimize the side reactions between the cycled electrodes and

electrolyte, then carefully washed by dimethyl carbonate solvent to remove the soluble surface species. All the dried electrodes were prepared inside an Ar-filled glove box (H_2O < 0.1 ppm) to avoid air exposure. The electron microscopy work was carried out with JEOL JEM-2100F and Hitachi HD2700C dedicated STEM with probe corrector at an accelerating voltage of 200 kV. Atomic resolution HAADF-STEM images were filtered using Digital Micrograph software.

Electrochemical Characterization. Electrodes were prepared from slurries containing 80 wt% of active material, 10 wt% of polyvinylidene fluoride (PVdF) binder, and 10 wt% acetylene carbon black (Denka, 50% compressed) in N-methylpyrrolidone (NMP) solvent. The slurries were casted on the carbon-coated aluminum current collectors (Exopack Advanced Coatings) using a doctor blade, then dried under vacuum at 120 ºC overnight. Typical loadings of the active materials were ~2.5 mg cm^{-2}. 2032-type coin cells (Hohsen Corp.) containing Li metal, a Celgard 2400 separator, and 1M $LiPF_6$ electrolyte solution in 1:2 w/w ethylene carbonate - diethyl carbonate (Daikan American, Inc.) were assembled inside an Ar-filled glove box (H_2O < 0.1 ppm). Galvanostatic discharge and charge testing was performed on a Maccor 4200 cycler at 5 mA g^{-1}, unless noted otherwise, between 4.6 V and 2.0 V. 1C capacity was defined as 250 mAh g^{-1}.

Characterization of Oxygen State. mRIXS maps were collected in high-efficiency iRIXS endstation at Beamline 8.0.1 at ALS in Lawrence Berkeley National Laboratory.[2] Samples were prepared under Ar through a home-made sample transfer kit throughout the handling process without any air exposure. RIXS resolving power and other technical details could be found in our previous report.[3-4] The *operando* DEMS measurement was conducted using a customized Swagelok type cell such that the cell headspace was periodically swept to a mass spectrometer. The details were described in previous publications.[3, 5] DEMS electrodes were prepared by mixing 80 wt% active material, 10 wt% polytetrafluoroethylene (PTFE), and 10 wt% acetylene carbon

black prior to being pressed onto stainless steel mesh. Other cell components were identical to those used in the electrochemical tests. DEMS measurements were performed by initially allowing the cell to rest at open circuit voltage to establish a baseline for CO_2 and O_2 mass spectrometer ion currents, followed by charge/discharge at constant current using a Bio-Logic SP-300 potentiostat.

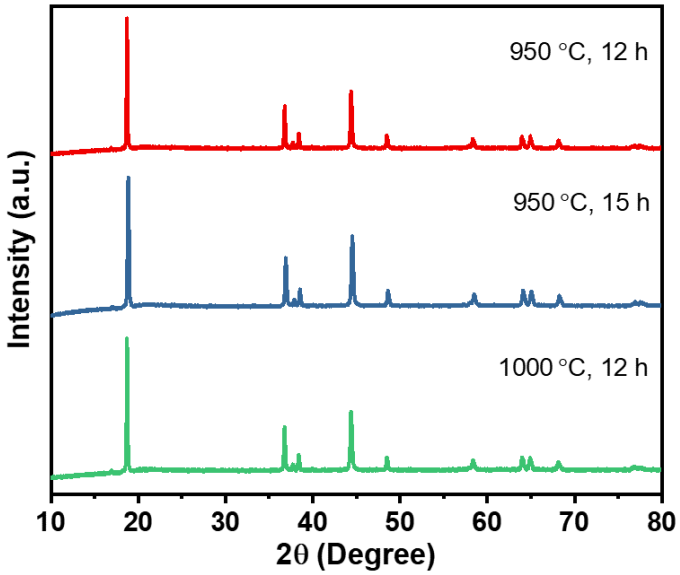

Figure S1. XRD patterns of LRCO synthesized at different conditions.

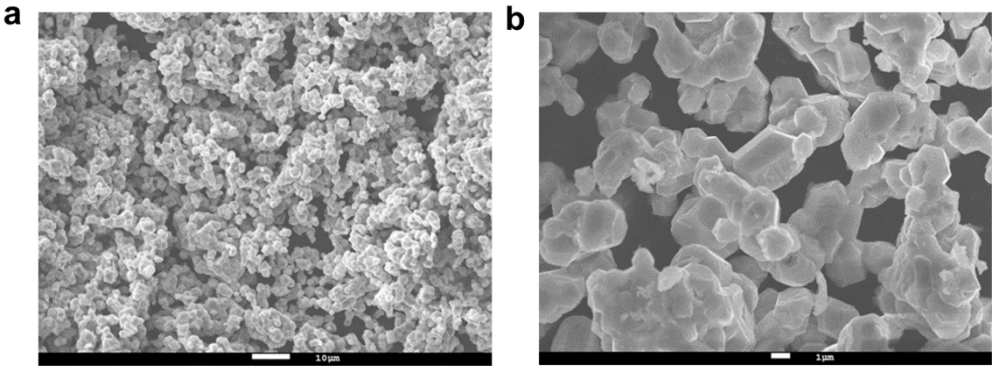

Figure S2. SEM images of LRCO sample synthesized at 950 ºC for 15 h, scale bar in (a) and (b) is 10 and 1 µm, respectively.

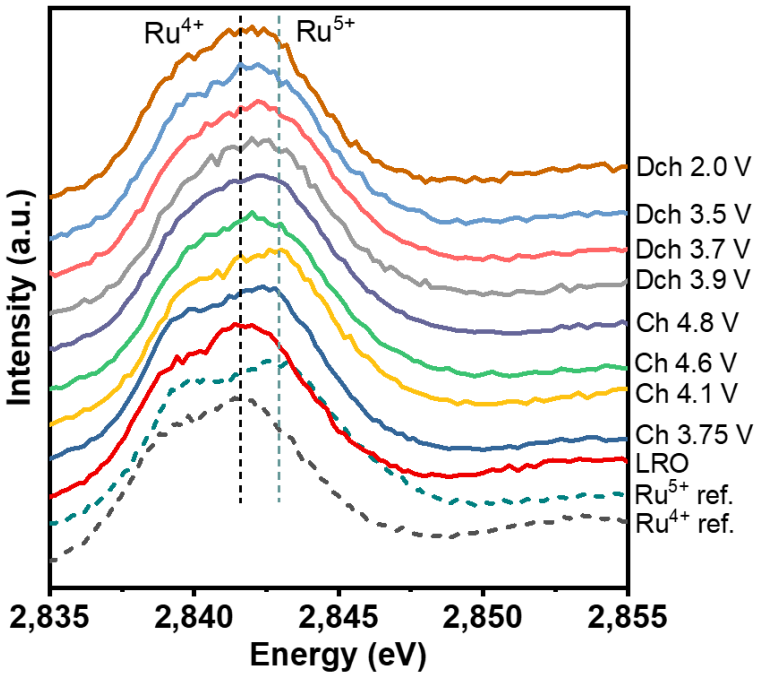

Figure S3. Ru *L*-edge tender XAS of LRCO material at different states of charge.

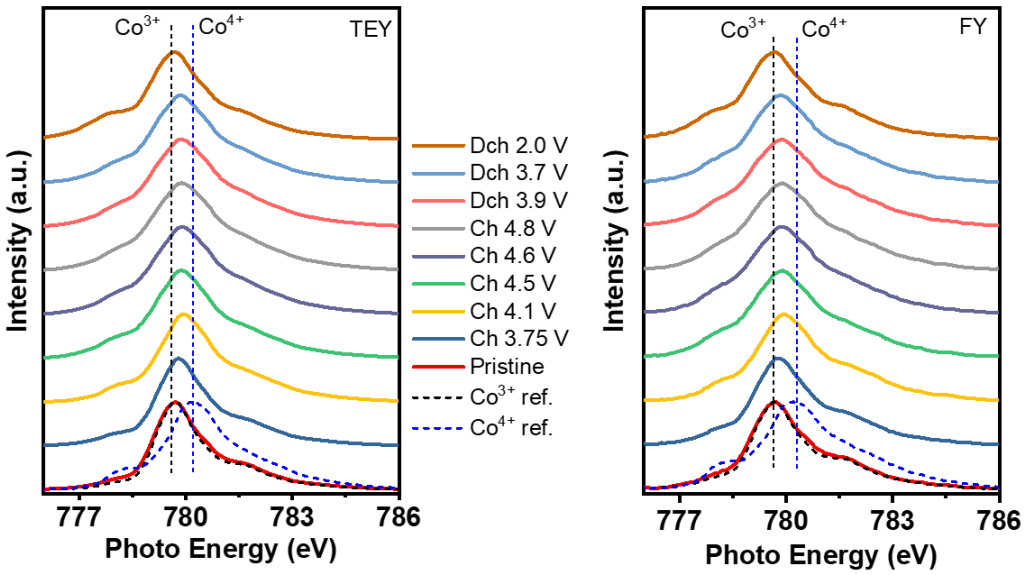

Figure S4. Co *L*-edge XAS of LRCO material at different states of charge.

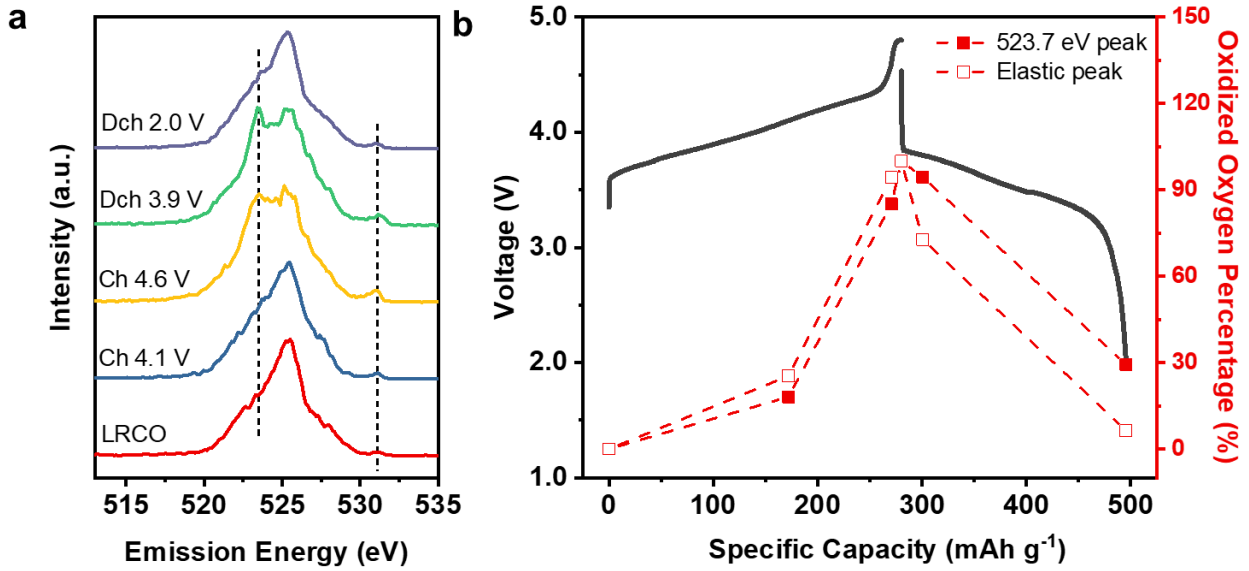

Figure S5. O redox characterization and contribution to capacity of LRCO. (a) RIXS cut of O *K*-edge at excitation energy of 531.0 eV, showing O redox evolution via fingerprinting peak at emission energy of 523.0 eV and elastic peak at emission energy of 531.0 eV; and (b) the first charge-discharge voltage profile along with the contribution of O redox at different states of charge estimated from the fingerprinting O redox and elastic peaks highlighted in (a).

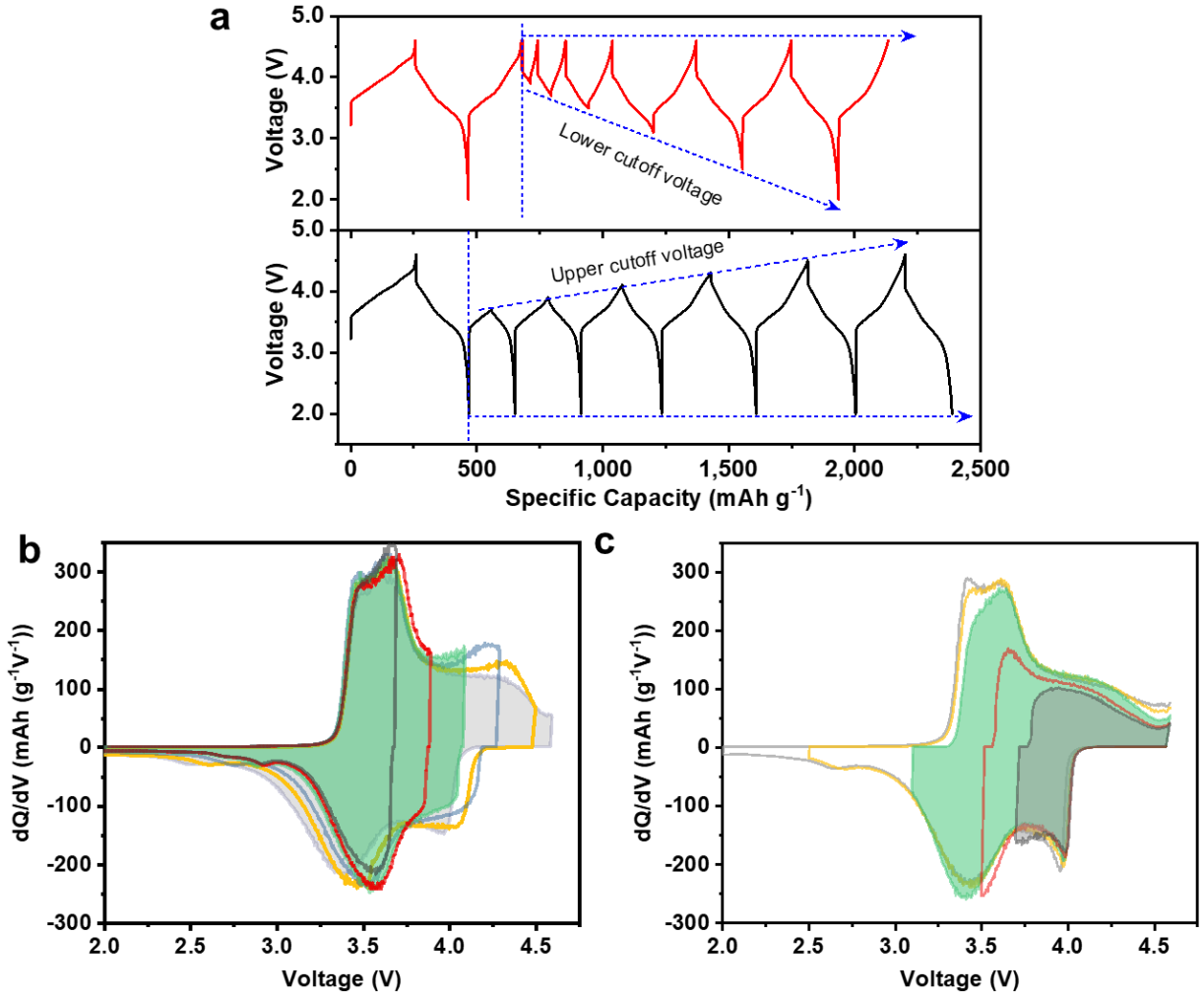

Figure S6. Electrochemical characterization on redox processes. (a) The charge-discharge voltage profiles and the corresponding dQ/dV plots at different (b) charge cutoff voltages and (c) discharge cutoff voltages of LRCO material. Cells are cycled between 4.6 and 2 V at C/20.

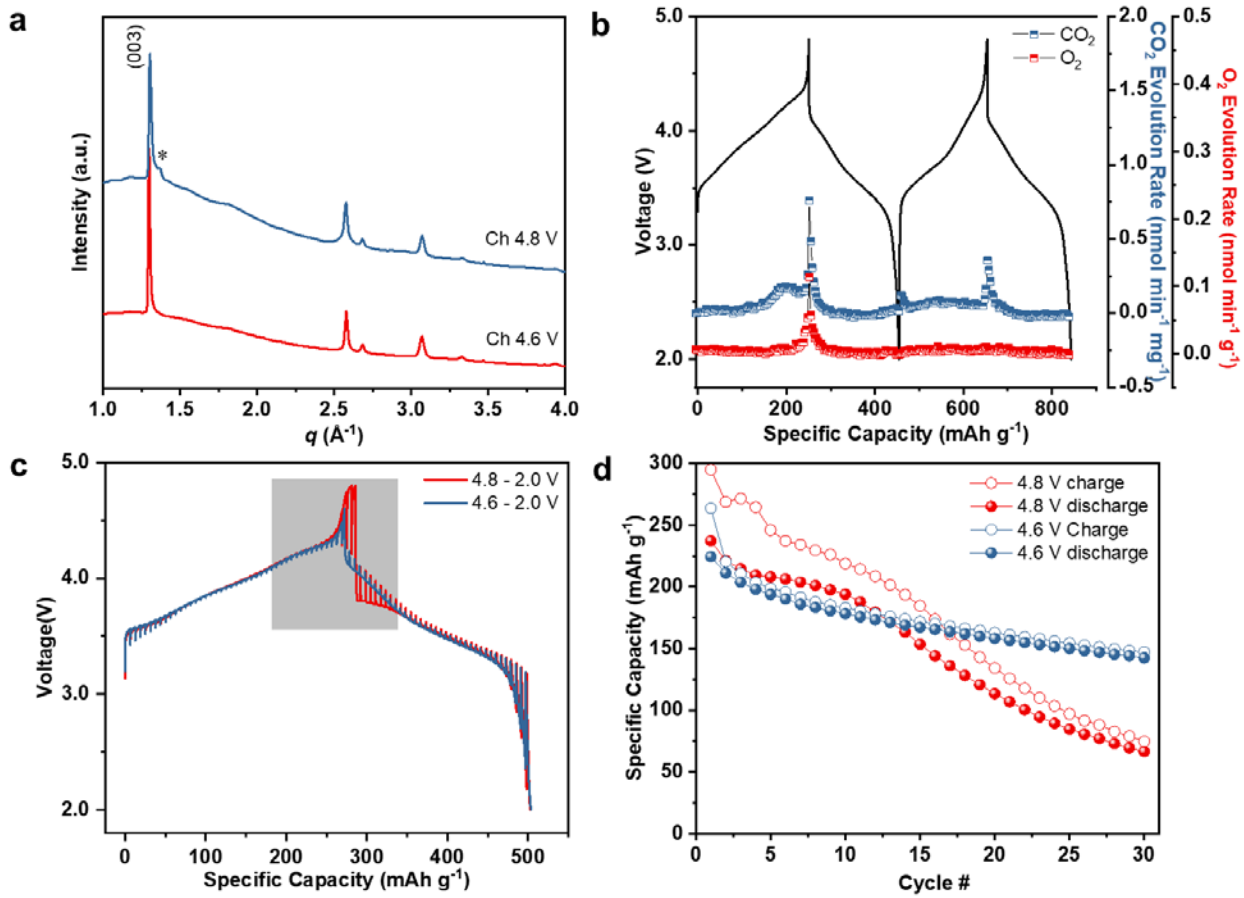

Figure S7. Electrochemical behaviors of LRCO at high voltages. (a) *Ex situ* WAXS at 4.6 and 4.8 V charge, phase transition is evidenced by a shoulder peak around (003) above 4.6 V; (b) gas evolution analysis by operando DEMS at 4.8 V charge cutoff voltage, with the onset voltage of CO_2 (carbonate residual) and O_2 evolution around 3.9 and 4.3 V, respectively, the total O_2 gas release is 0.07 mol% of all O in LRCO; (c) GITT tests between 4.6 – 2.0 V and 4.8 – 2.0 V, showing the oxidation reaction at 4.6 – 4.8 V has a significant impact on the kinetics of the initial reduction reaction but not those in the middle to low voltage range; (d) cycling performance at 4.8 – 2.0 V and 4.6 – 2.0 V, showing a relatively large increase in charge capacity but little on discharge capacity, the large irreversible capacity at 4.8 V cycling indicates severe parasitic reactions above 4.8 V.

Table S1: Refined structural parameters of sXRD for LRCO based on $R\bar{3}m$.

Atom	Wyckoff	x	y	z	Occupancy	Uiso
O	6	0	0	0.25792(7)	1	0.0040
Li1	3	0	0	0.5	1	0.00289
Ru	3	0	0	0	0.4	0.00414
Co	3	0	0	0	0.4	0.00414
Li2	3	0	0	0	0.2	0.00414

Lattice parameter: $a = b = 2.8798(2)$ Å, $c = 14.376(1)$ Å, $\alpha = \beta = 90^{o}$, $\gamma = 120^{o}$, $R_p = 9.81\%$.

References

1. Toby, B., EXPGUI, A Graphical User Interface for GSAS. *J. Appl. Crystallogr.* **2001,** *34* (2), 210-213.
2. Qiao, R.; Li, Q.; Zhuo, Z.; Sallis, S.; Fuchs, O.; Blum, M.; Weinhardt, L.; Heske, C.; Pepper, J.; Jones, M.; Brown, A.; Spucces, A.; Chow, K.; Smith, B.; Glans, P.-A.; Chen, Y.; Yan, S.; Pan, F.; Piper, L. F. J.; Denlinger, J.; Guo, J.; Hussain, Z.; Chuang, Y.-D.; Yang, W., High-Efficiency in situ Resonant Inelastic X-ray Scattering (iRIXS) Endstation at the Advanced Light Source. *Rev. Sci. Instrum.* **2017,** *88* (3), 033106.
3. Xu, J.; Sun, M.; Qiao, R.; Renfrew, S. E.; Ma, L.; Wu, T.; Hwang, S.; Nordlund, D.; Su, D.; Amine, K.; Lu, J.; McCloskey, B. D.; Yang, W.; Tong, W., Elucidating Anionic Oxygen Activity in Lithium-Rich Layered Oxides. *Nat. Commun.* **2018,** *9* (1), 947.
4. Gent, W. E.; Lim, K.; Liang, Y.; Li, Q.; Barnes, T.; Ahn, S.-J.; Stone, K. H.; McIntire, M.; Hong, J.; Song, J. H., Coupling between Oxygen Redox and Cation Migration Explains Unusual Electrochemistry in Lithium-Rich Layered Oxides. *Nat. Commun.* **2017,** *8* (1), 2091.
5. Renfrew, S. E.; McCloskey, B. D., Residual Lithium Carbonate Predominantly Accounts for First Cycle CO_2 and CO Outgassing of Li-Stoichiometric and Li-Rich Layered Transition-Metal Oxides. *J. Am. Chem. Soc.* **2017,** *139* (49), 17853-17860.